Theory of solar cell light trapping through a nonequilibrium Green's function formulation of Maxwell's equations

Siddharth Buddhiraju and Shanhui Fan

Phys. Rev. B **96**, 035304 — Published 14 July 2017

DOI: 10.1103/PhysRevB.96.035304

Theory of Solar Cell Light-Trapping through a Non-Equilibrium Green's Function formulation of Maxwell's Equations

Siddharth Buddhiraju[1] and Shanhui Fan[1]

[1] *Ginzton Laboratory, Department of Electrical Engineering, Stanford University, Stanford, California 94305, USA*

(Dated: June 19, 2017)

We develop a theory of solar cell light trapping based on directly solving Maxwell's equations through a non-equilibrium Green's function formalism. This theory rigorously connects the maximum power absorbed by the solar cell to the density of states of the cell. With this theory we are able to reproduce all standard results in solar cell light trapping previously derived using approximate formalisms. Therefore our development places solar cell light trapping theory on a much firmer theoretical foundation. Moreover, here the maximum power formula is derived without the assumption of reciprocity, unlike all previous theories on solar cell light trapping. Therefore, we prove that the upper bound of light trapping enhancement cannot be overcome with the use of non-reciprocal structures. As a numerical test, we simulate an absorber structure that consists of a non-reciprocal material, and show that the absorption enhancement factor is largely independent of non-reciprocity, in consistency with the theory.

I. INTRODUCTION

For practical solar cell design, various techniques of light trapping have been widely applied in order to achieve near-complete absorption of sunlight using a cell with a thickness that is smaller than the absorption depth of the material [1–23]. The use of light trapping can reduce the amount of material used in a solar cell and hence reduce the cost of solar energy. In addition, the use of a thinner cell without sacrificing absorption capability enhances carrier exaction and therefore the efficiency of the solar cell [24].

The practical importance of light trapping in solar cells, in turn, has motivated a significant body of theoretical works aiming to understand the fundamental limits of absorption enhancement that can be achieved with light trapping techniques. Ref. [1] considered the theoretical limits for light trapping in standard crystalline silicon cells. Using an argument combining ray optics with thermodynamics, it was shown that compared to a single-pass absorption coefficient, light trapping induced by a Lambertian surface roughness can enhance the absorption by a factor of $4n^2$ when the single-pass absorption is negligible, where n is the refractive index of silicon. For cells with emission restricted to a cone with an apex angle of θ, the enhancement factor can be further improved to $4n^2/\sin^2\theta$, again for a material with infinitesimal loss [3]. The effect of more realistic material absorption on light trapping has been considered in Ref. [25], which shows that in general the light trapping enhancement factor goes down as the material absorption increases. These classic papers form the foundation of light trapping theory for solar cells and have had substantial influence on the optical design of crystalline silicon cells.

Since the thickness of crystalline silicon cell is typically on the order of 50-100 microns [4], and the roughness used for light trapping has a length scale on the order of 10s of microns, the optical properties of standard crystalline silicon cell can be well described by the ray optics model. On the other hand, in recent years there has been significant interest in the study of nanophotonic solar cells, where both the thickness of the cell and the size of features used for light trapping purposes are on a single-wavelength or even deep sub-wavelength scale [7–12, 14–16, 18, 20]. For these structures, ray optics theory is no longer applicable. Therefore, there have in parallel been substantial developments seeking to formulate light trapping theory instead from an electromagnetic point of view [26–30]. In particular, in Refs. [28–30] a statistical coupled mode theory formalism for light trapping in solar cells was developed. Using this formalism, the standard results of light trapping in crystalline silicon solar cells as previously derived with ray optics could be reproduced. Moreover, it was predicted that in the nanophotonic regime, the $4n^2$ limit could be significantly overcome through nanoscale modal confinement over broad bandwidths. Related to these works, it was discussed in Ref. [31] that the light trapping enhancement factor can be related to the local density of electromagnetic modes.

The coupled mode theory formalism that underlies the work of Refs. [28–30], however, is an approximate formalism. While it is very well justified especially when considering the coupling of external light with a structure containing only a few modes [32–34], in a solar cell system one needs to consider a large number of optical modes. In order to place the theory of light trapping in nanophotonic structures on a firmer theoretical foundation, it is therefore of fundamental importance to formulate the problem of light trapping directly from Maxwell's equations.

In this paper, we develop a theory of light trapping directly from Maxwell's equations. For this purpose, we adapt the Non-Equilibrium Green's Function (NEGF) formalism [35, 36], which has been widely used in studying transport in nanoscale electronic systems, for Maxwell's equations. Our theory provides a rigorous proof of the connection of light trapping enhancement factor to the Density of States (DOS) of the device. This connection can then be used to reproduce the standard predictions of light trapping theory. Moreover, as a key theoretical advancement, the proof here does not use reciprocity or detailed balance. This is in contrast to Ref. [28] where the underlying temporal coupled mode theory formalism is derived using the assumption of reciprocity. It is also in contrast with Ref. [1] which uses a detailed balance argument that is equivalent to reciprocity. Consequently, our theory shows that introducing non-reciprocity alone does not enhance the limit of light trapping. We validate this theoretical prediction by a direct numerical simulation.

This paper is organized as follows: In Section II, we setup the solar cell problem, discuss the statistical nature of the incident solar radiation, and derive an expression for the absorbed power. In Section III, we apply the NEGF formalism to this setup, and derive relations regarding the density of states of the device. In Section IV, we combine these formalisms to derive the power absorbed by a near-lossless solar cell under incident sunlight. In Section V, we use the formalism to reproduce the standard results of light trapping theory. In Section VI, we discuss light trapping in non-reciprocal structures, and provide a numerical test of our theory. In Section VII, we extend the theory to materials where the loss is not infinitesimal. We finally conclude in Section VIII.

II. THE SOLAR CELL PROBLEM

The device under consideration in this work is a solar cell with an arbitrary geometry. The cell surface may be patterned with gratings [8, 28] or textured [4, 37] to enhance coupling with incident radiation. Fig. 1(a) depicts a typical solar cell setup, with the orange arrow representing solar radiation incident from a narrow angular range and the green arrows representing a broad angular emission. A rear-reflector increases the path length of the light inside the cell. Fig. 1(b) describes a theoretically simpler problem to study, which corresponds to a concentrated, isotropic source in the upper half-space, and isotropic emission from the cell in the upper half-space. Fig. 1(b) is theoretically related to Fig. 1(c), which depicts a solar cell with an isotropic emission in the presence of an isotropic source.

The solar radiation incident on the cell can be described by a stationary random process, such that the ensemble average of the incident electric and magnetic fields are time-independent. Therefore, the field-field

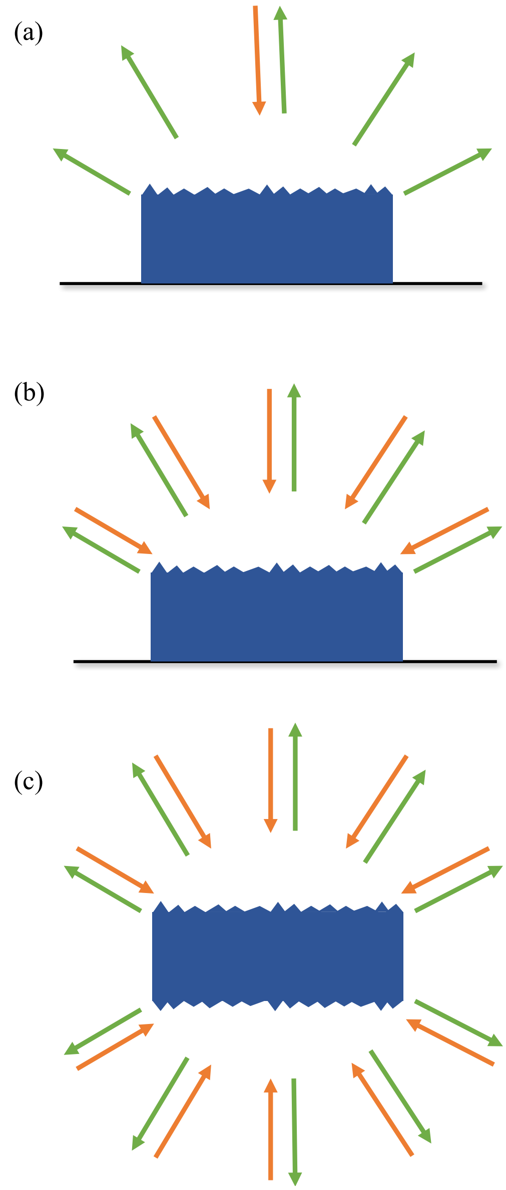

FIG. 1. (a) A typical cell operating under solar radiation that covers a narrow angular range (orange). The cell surfaces may be patterned to enhance coupling with incident radiation. The emission from the cell has a broad-angular (green) response. A rear reflector is usually placed underneath such a cell to enhance absorption. (b) The same cell under concentrated, near-isotropic incident radiation from the upper half-space and near-isotropic emission into the upper half-space. (c) A setup theoretically related to (b), with a near-isotropic incident radiation as well as emission from the cell.

correlation for the incident electric field $\mathbf{E}_\mathrm{I}$ is given by $\left\langle \mathbf{E}_\mathrm{I}(\mathbf{r},\omega)\mathbf{E}_\mathrm{I}^\dagger(\mathbf{r}',\omega')\right\rangle = 2\pi\delta(\omega-\omega')\left\langle \mathbf{E}_\mathrm{I}(\mathbf{r})\mathbf{E}_\mathrm{I}^\dagger(\mathbf{r}')\right\rangle_\omega$ where the $\delta(\omega-\omega')$ term appears because of stationarity. In this paper, the $\dagger$ superscript refers to a conjugate transpose, while the T superscript refers to only a transpose.

Since the cell receives this stationary input field, the electric field in the device, $\mathbf{E}_\mathrm{D}(t)$, is also described by a stationary random process with a field-field correlation function

$$\langle \mathbf{E}_\mathrm{D}(\mathbf{r},\omega)\mathbf{E}_\mathrm{D}^\dagger(\mathbf{r}',\omega')\rangle = 2\pi\delta(\omega-\omega')\langle \mathbf{E}_\mathrm{D}(\mathbf{r})\mathbf{E}_\mathrm{D}^\dagger(\mathbf{r}')\rangle_\omega \quad (1)$$

The ensemble-averaged power absorbed by the cell can then be determined from Poynting's theorem (Ref. [38] p. 259) in the absence of any currents:

$$\oint \mathrm{d}\mathbf{S}\cdot\langle \mathbf{E}_\mathrm{D}\times\mathbf{H}_\mathrm{D}\rangle = - \int \mathrm{d}V \Big\langle \mathbf{E}_\mathrm{D}(\mathbf{r})\cdot\frac{\partial \mathbf{D}_\mathrm{D}(\mathbf{r})}{\partial t} + \mathbf{H}_\mathrm{D}(\mathbf{r})\cdot\frac{\partial \mathbf{B}_\mathrm{D}(\mathbf{r})}{\partial t}\Big\rangle \quad (2)$$

A non-zero value of the left hand side would indicate a net flow of power into the cell, i.e. absorption in the cell. We evaluate the first term on the right hand side of Eq. (2) as follows:

$$P = -\int dV \Big\langle \mathbf{E}_\mathrm{D}(\mathbf{r})\cdot\frac{\partial \mathbf{D}_\mathrm{D}(\mathbf{r})}{\partial t}\Big\rangle \quad (3)$$

$$= \int dV \int\int_{-\infty}^{\infty} \frac{d\omega'}{2\pi}\frac{d\omega}{2\pi}\langle \mathbf{E}_\mathrm{D}(\mathbf{r},\omega)\cdot i\omega'\mathbf{D}_\mathrm{D}^*(\mathbf{r},\omega')\rangle e^{i(\omega-\omega')t} \quad (4)$$

$$= \int_{-\infty}^{\infty}\int_{-\infty}^{\infty} \frac{d\omega' d\omega}{(2\pi)^2} i\omega' \,\mathrm{Tr}\,\langle \mathbf{E}_\mathrm{D}(\omega)\mathbf{D}_\mathrm{D}^\dagger(\omega')\rangle e^{i(\omega-\omega')t} \quad (5)$$

$$= \int_{-\infty}^{\infty}\int_{-\infty}^{\infty} \frac{d\omega' d\omega}{(2\pi)^2} i\omega' \,\mathrm{Tr}\left[\epsilon^\dagger(\omega)\langle \mathbf{E}_\mathrm{D}(\omega)\mathbf{E}_\mathrm{D}^\dagger(\omega')\rangle\right] e^{i(\omega-\omega')t} \quad (6)$$

$$= \int_{-\infty}^{\infty} \frac{d\omega}{2\pi} i\omega \,\mathrm{Tr}\left[\epsilon^\dagger(\omega)\langle \mathbf{E}_\mathrm{D}\mathbf{E}_\mathrm{D}^\dagger\rangle_\omega\right] \quad (7)$$

$$= \int_{0}^{\infty} \frac{d\omega}{2\pi} i\omega \,\mathrm{Tr}\left[(\epsilon^\dagger(\omega)-\epsilon(\omega))\langle \mathbf{E}_\mathrm{D}\mathbf{E}_\mathrm{D}^\dagger\rangle_\omega\right] \quad (8)$$

$$= \int_{0}^{\infty} \frac{d\omega}{\pi} \omega \,\mathrm{Tr}\left[\mathrm{Im}\,\epsilon(\omega)\langle \mathbf{E}_\mathrm{D}\mathbf{E}_\mathrm{D}^\dagger\rangle_\omega\right] \quad (9)$$

Note that in Eqs. (2)-(3), the fields are the underlying physical, time-dependent fields that are real, whereas in the rest of the paper, the fields are complex phasors.

In obtaining Eq. (5), we use $\mathbf{E}_\mathrm{D}(\omega)$ to represent a column vector, which, when all indices are explicitly shown, denotes $\mathbf{E}_{\mathrm{D},m}(\mathbf{r},\omega)$, where m denotes the indices for the polarization. $\mathbf{E}_\mathrm{D}(\omega)\mathbf{D}_\mathrm{D}^\dagger(\omega')$ therefore represents a *tensorial* quantity, which corresponds to $\mathbf{E}_{\mathrm{D},m}(\mathbf{r},\omega)\mathbf{D}_{\mathrm{D},n}^\dagger(\mathbf{r}',\omega')$, where m and n again denote the polarization index. For any tensorial quantity $\mathbb{A} \equiv A_{mn}(\mathbf{r},\mathbf{r}')$, the trace operator Tr is defined as:

$$\mathrm{Tr}\,\mathbb{A} \equiv \sum_m \int dV A_{mm}(\mathbf{r},\mathbf{r}) \quad (10)$$

That is, the operator $\mathbb{A}$ can be considered a large matrix indexed both in polarization and position. The Tr operation is then simply the sum of the diagonal elements of the matrix. For the continuous position coordinate, this sum is in fact an integral over the volume of the device. For the rest of the paper, we will be using such vector and tensor quantities whenever we do not explicitly exhibit the coordinate and polarization indices.

Next, we used Eq. (1) to obtain Eq. (7). To obtain Eq. (8), we use the fact that because the underlying fields $\mathbf{E}(\mathbf{r},t)$ and $\mathbf{D}(\mathbf{r},t)$ are real, $\epsilon^*(-\omega)=\epsilon(\omega)$ and $\mathbf{E}^*(-\omega)=\mathbf{E}(\omega)$ (Ref. [38] p. 262).

With a similar derivation, one can show that the second term on the right-hand side of Eq. (2) is zero since we assume the permeability to be μ_0 with no imaginary part.

In order to compute the absorption of the solar cell, we need to relate the fields inside the device $\mathbf{E}_\mathrm{D}$, to the incident solar radiation $\mathbf{E}_\mathrm{I}$. This relation is obtained from the Non-Equilibrium Green's Function (NEGF) formalism in the next section.

III. NEGF FORMULATION FOR A LOSSLESS SYSTEM

Certainly, the materials used in solar cells are absorptive, and therefore are described by a dielectric function $\epsilon(\mathbf{r})$ with a non-zero imaginary part. However, in the understanding of light trapping theory, the computation of the enhancement factor when the material loss is infinitesimal plays a significant role [1, 4, 28, 39]. Therefore, in this paper we will start by considering the case where the material absorption is infinitesimal. The formalism that we develop here, however, can be generalized to treat the case where the material absorption is non-negligible, which we will discuss in Section VII.

To compute the absorption enhancement factor where the material absorption is infinitesimal, in this section we consider the corresponding lossless system as described by the real part $\epsilon_\mathrm{R}(\mathbf{r})$ of the dielectric function $\epsilon(\mathbf{r})$ i.e. $\epsilon_\mathrm{R}(\mathbf{r}) = \mathrm{Re}[\epsilon(\mathbf{r})]$, and describe the electromagnetic structure and the coupling of externally incident waves to such a system. In the next section we then relate the absorption properties of the system with infinitesimal loss to such a lossless system.

Further, for simplicity, we ignore material dispersion in the real part of the dielectric function, i.e. $\epsilon_\mathrm{R}(\mathbf{r},\omega) = \epsilon_\mathrm{R}(\mathbf{r})$. This simplification is justified since for light-trapping purposes, one typically considers a frequency range near the semiconductor band-edge where the variation in the real part of the dielectric function, i.e. in $\epsilon_{\rm R}(\mathbf{r},\omega)$, is usually small. In addition, we restrict $\epsilon_{\rm R}(\mathbf{r})$ to be positive definite, which is applicable for typical semiconductors. However, we note that both the material dispersion and the negative dielectric constant cases can be treated in a similar fashion to what we consider here by an auxiliary field approach [40]. With this approach, one can formulate the modal structure of a dispersive medium as a standard eigenvalue problem where the system matrix has no explicit frequency dependence. Therefore, the formalism that we develop here can be generalized for systems such as plasmonics-enhanced solar cells [11].

Consider the Maxwell's Equations in frequency domain for a system described by $\epsilon_{\rm R}$:

$$\nabla \times \mathbf{E}(\omega) = -i\omega \mathbf{B}(\omega) \tag{11}$$

$$\nabla \times \mathbf{H}(\omega) = i\omega \mathbf{D}(\omega) \tag{12}$$

with the constitutive relations

$$\mathbf{B}(\omega) = \mu_0 \mathbf{H}(\omega) \tag{13}$$

$$\mathbf{D}(\omega) = \epsilon_0 \epsilon_{\rm R} \mathbf{E}(\omega) \tag{14}$$

Since $\epsilon_{\rm R}$ is positive semi-definite, a positive semi-definite square-root $\sqrt{\epsilon_{\rm R}}$ exists, and Eqs. (11) to (14) can be combined to form a Hermitian eigenvalue problem [41]:

$$\mathbb{H}\mathbf{F} = \left[\sqrt{\epsilon_{\rm R}^{-1}}\nabla \times \nabla \times \sqrt{\epsilon_{\rm R}^{-1}}\right]\mathbf{F} = \frac{\omega^2}{c^2}\mathbf{F} \tag{15}$$

where $\mathbf{F} = \sqrt{\epsilon_{\rm R}}\mathbf{E}$. To make a connection to the standard NEGF literature, we refer to the operator $\mathbb{H}$ defined above as the 'Hamiltonian' of the system.

We now apply Eq. (15) to the system containing both the cell itself, as well as the surrounding air regions that have a uniform $\epsilon = 1$. The following derivation is based largely on Ref. [35], starting p. 188, and its results are summarized in Ref. [35] p. 223. The readers are referred to Ref. [35] for a detailed discussion of the concepts in this section, and to Ref. [42] for a more formal treatment of NEGF.

The Hamiltonian of the system, $\mathbb{H}$, can be decomposed as

$$\mathbb{H} = \begin{pmatrix} \mathbb{H}_{\rm S} & \tau^\dagger \\ \tau & \mathbb{H}_{\rm D} \end{pmatrix} \tag{16}$$

where $\mathbb{H}_{\rm S}$ and $\mathbb{H}_{\rm D}$ are the Hamiltonians of the surroundings and the cell, respectively. The off-diagonal terms τ and $\tau^\dagger$ can be numerically obtained, for example, by explicitly constructing $\mathbb{H}$ in Eq. (15) by discretizing the spatial coordinates $\mathbf{r}$. We note that τ is in general not equal to $\tau^\dagger$. In other words, $\mathbb{H}$ might not be a symmetric matrix, and therefore we do not assume reciprocity in this derivation. Using Eq. (16), Eq. (15) can be rewritten as

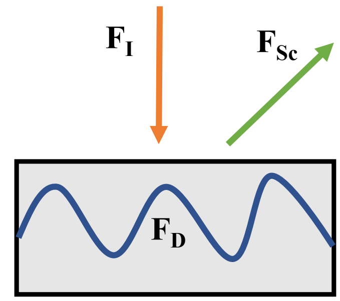

FIG. 2. An illustration of Eq. (17). The incident field $\mathbf{F}_{\rm I}$ is scattered in general into the scattered field $\mathbf{F}_{\rm Sc}$ at the boundary, and generates the device field $\mathbf{F}_{\rm D}$.

$$\begin{pmatrix} (\frac{\omega}{c})^2 - \mathbb{H}_{\rm S} & -\tau^\dagger \\ -\tau & (\frac{\omega}{c})^2 - \mathbb{H}_{\rm D} \end{pmatrix} \begin{pmatrix} \mathbf{F}_{\rm I} + \mathbf{F}_{\rm Sc} \\ \mathbf{F}_{\rm D} \end{pmatrix} = \mathbf{0} \tag{17}$$

where $\mathbf{F} = (\mathbf{F}_{\rm I} + \mathbf{F}_{\rm Sc}, \mathbf{F}_{\rm D})^T$ is an eigenvector of $\mathbb{H}$. The subscripts of $\mathbf{F}$ are used to distinguish components of $\mathbf{F}$: $\mathbf{F}_{\rm I}$ is the field incident from the surroundings onto the device (solar cell), $\mathbf{F}_{\rm Sc}$ is the scattered field from the device back into the surroundings, and $\mathbf{F}_{\rm D}$ is the field in the device. Fig. 2 depicts the incident, scattered and the device fields as described here.

An expression for the field in the device $\mathbf{F}_{\rm D}$ can be obtained by solving Eq. (17). To do this, we first note that the incident field $\mathbf{F}_{\rm I}$ satisfies $\big[(\frac{\omega}{c})^2 - \mathbb{H}_{\rm S}\big]\mathbf{F}_{\rm I} = 0$. Therefore from the first row of Eq. (17), $\big[(\frac{\omega}{c})^2 - \mathbb{H}_{\rm S}\big]\mathbf{F}_{\rm Sc} - \tau^\dagger \mathbf{F}_{\rm D} = 0$, so that

$$\mathbf{F}_{\rm Sc} = \mathbb{G}_{\rm S}\tau^\dagger \mathbf{F}_{\rm D} \tag{18}$$

where $\mathbb{G}_{\rm S} = \big[(\frac{\omega}{c})^2 - \mathbb{H}_{\rm S} - i\eta\big]^{-1}$ with η being an infinitesimal positive number, is the retarded Green's function for the free space surrounding the device. Note that the retarded Green's function contains a $-\eta$ here, in contrast with $+\eta$ in Ref. [35] due to the $+i\omega t$ convention used here as opposed to the $-i\omega t$ convention in quantum mechanics. From the second row of Eq. (17), $\big[(\frac{\omega}{c})^2 - \mathbb{H}_{\rm D}\big]\mathbf{F}_{\rm D} - \tau(\mathbf{F}_{\rm I} + \mathbf{F}_{\rm Sc}) = 0$, which gives

$$\big[(\frac{\omega}{c})^2 - \mathbb{H}_{\rm D} - \Sigma)\big]\mathbf{F}_{\rm D} = \tau \mathbf{F}_{\rm I} \tag{19}$$

where $\Sigma = \tau \mathbb{G}_{\rm S} \tau^\dagger$ is the self-energy. Eq. (19) can be succinctly written as

$$\mathbf{F}_{\rm D} = \mathbb{G}_{\rm D}\tau \mathbf{F}_{\rm I} \tag{20}$$

where we identify

$$\mathbb{G}_{\rm D} = \big[(\frac{\omega}{c})^2 - \mathbb{H}_{\rm D} - \Sigma\big]^{-1} \tag{21}$$

as the effective Green's function for the device coupled to its environment.

Before we provide a discussion of the density of states of the device under consideration, we consider the density of states of a closed system. Consider the Green's function for a general system with Hamiltonian $\mathbb{H}$, $\mathbb{G} = \left[(\frac{\omega}{c})^2 - \mathbb{H} - i\eta\right]^{-1}$. From the equation $\mathbb{H}\mathbf{F}^{(m)} = (\omega_m^2/c^2)\mathbf{F}^{(m)}$, we have the retarded Green's function

$$\mathbb{G} = c^2 \sum_m \frac{\mathbf{F}^{(m)}\mathbf{F}^{(m)\dagger}}{\omega^2 - \omega_m^2 - i\eta} \tag{22}$$

The density of states is related to $\operatorname{Im}\mathbb{G}$, which from Eq. (22), is given by

$$\begin{aligned}\frac{1}{\pi}\operatorname{Im}\mathbb{G} &= c^2 \sum_m \delta(\omega^2 - \omega_m^2)\mathbf{F}^{(m)}\mathbf{F}^{(m)\dagger} \\ &= c^2 \sum_m \frac{1}{2\omega_m}\delta(\omega - \omega_m)\mathbf{F}^{(m)}\mathbf{F}^{(m)\dagger} \\ &= c^2 \sum_m \frac{1}{2\omega}\delta(\omega - \omega_m)\mathbf{F}^{(m)}\mathbf{F}^{(m)\dagger}\end{aligned} \tag{23}$$

which gives us the relation

$$\mathbb{A} \equiv \sum_m \delta(\omega - \omega_m)\mathbf{F}^{(m)}\mathbf{F}^{(m)\dagger} = \frac{2\omega}{\pi c^2}\operatorname{Im}\mathbb{G} \tag{24}$$

where following the nomenclature of NEGF [35], $\mathbb{A}$ is called the spectral function. Note that we dropped the negative frequency solutions $-\omega_m$ in the summation since we are interested only in an integration over positive frequencies in Eq. (9). The local density of states (LDOS) $\rho(\mathbf{r})$ is given by [43]

$$\begin{aligned}\rho(\mathbf{r}) &\equiv \sum_{i=1}^{3} \mathbb{A}_{ii}(\mathbf{r}, \mathbf{r}) \\ &= \sum_m \delta(\omega - \omega_m)\mathbf{E}^{(m)*}(\mathbf{r}) \cdot \epsilon_{\mathrm{R}}(\mathbf{r})\mathbf{E}^{(m)}(\mathbf{r})\end{aligned} \tag{25}$$

Generalizing from the discussion above for the LDOS of a closed system, we define a spectral function specific to the device, given by

$$\mathbb{A}_{\mathrm{D}} = \frac{2\omega}{\pi c^2}\operatorname{Im}\mathbb{G}_{\mathrm{D}} \tag{26}$$

where $\mathbb{G}_{\mathrm{D}}$ is defined by Eq. (21). Eq. (26) can be manipulated to form a useful identity [35] using the following relation:

$$\begin{aligned}\operatorname{Im}\mathbb{G}_{\mathrm{D}} &= \frac{1}{2i}(\mathbb{G}_{\mathrm{D}} - \mathbb{G}_{\mathrm{D}}^{\dagger}) \\ &= \frac{1}{2i}\mathbb{G}_{\mathrm{D}}(\mathbb{G}_{\mathrm{D}}^{\dagger -1} - \mathbb{G}_{\mathrm{D}}^{-1})\mathbb{G}_{\mathrm{D}}^{\dagger} \\ &= \frac{1}{2i}\mathbb{G}_{\mathrm{D}}(\frac{\omega^2}{c^2} - \mathbb{H}_{\mathrm{D}} - \Sigma^{\dagger} - \frac{\omega^2}{c^2} + \mathbb{H}_{\mathrm{D}} + \Sigma)\mathbb{G}_{\mathrm{D}}^{\dagger} \\ &= \frac{1}{2i}\mathbb{G}_{\mathrm{D}}(\Sigma - \Sigma^{\dagger})\mathbb{G}_{\mathrm{D}}^{\dagger} \\ &= \mathbb{G}_{\mathrm{D}}[\operatorname{Im}\Sigma]\mathbb{G}_{\mathrm{D}}^{\dagger} \\ &= \mathbb{G}_{\mathrm{D}}\tau[\operatorname{Im}\mathbb{G}_{\mathrm{S}}]\tau^{\dagger}\mathbb{G}_{\mathrm{D}}^{\dagger}\end{aligned} \tag{27}$$

since $\Sigma = \tau\mathbb{G}_{\mathrm{S}}\tau^{\dagger}$. Therefore,

$$\mathbb{A}_{\mathrm{D}} = \frac{2\omega}{\pi c^2}\mathbb{G}_{\mathrm{D}}\tau[\operatorname{Im}\mathbb{G}_{\mathrm{S}}]\tau^{\dagger}\mathbb{G}_{\mathrm{D}}^{\dagger} \tag{28}$$

$\mathbb{A}_{\mathrm{D}}(\mathbf{r}, \mathbf{r}, \omega)$ has the interpretation of the 'accessible' density of states. To see this, note that if Σ is zero, then $\mathbb{G}_{\mathrm{D}}$ is Hermitian, and therefore $\mathbb{A}_{\mathrm{D}} = 0$ from Eq. (26). This notion can be generalized: if a subset of modes do not couple with the surroundings, then Σ for those modes is zero, and $\mathbb{A}_{\mathrm{D}}$ corresponding to those modes is zero. Therefore, $\sum_m A_{mm,\mathrm{D}}(\mathbf{r}, \mathbf{r}, \omega)$ is the local density of device modes that can couple with the incident radiation. On the other hand, the full Green's function will consist of the decoupled surroundings and device Green's functions. Therefore, $\mathbb{G}$ over the device coordinates will simply be $\left[\omega^2/c^2 - \mathbb{H}_{\mathrm{D}} - i\eta\right]^{-1}$ and $\sum_m A_{mm}(\mathbf{r}, \mathbf{r}, \omega)$ will then be the device local density of states, regardless of whether these states actually couple to the incident radiation. This means that $\sum_m A_{mm,\mathrm{D}}(\mathbf{r}, \mathbf{r}, \omega)$ is in general lesser than or equal to the local density of states given by $\sum_m A_{mm}(\mathbf{r}, \mathbf{r}, \omega)$ corresponding to the isolated device, i.e.

$$\sum_m A_{mm,\mathrm{D}}(\mathbf{r}, \mathbf{r}, \omega) \leq \sum_m A_{mm}(\mathbf{r}, \mathbf{r}, \omega) \tag{29}$$

IV. ABSORPTION UNDER FULLY CONCENTRATED SUNLIGHT

We now have a mathematical structure to connect the device field $\mathbf{F}_{\mathrm{D}}$ to the incident field $\mathbf{F}_{\mathrm{I}}$ described through Eq. (20). We have also established the concept of LDOS defined through Eq. (26) and Eq. (28) for a lossless system. As a step forward, suppose the device has a small imaginary part of $\epsilon(\mathbf{r})$, i.e. $\operatorname{Im}(\epsilon)/\operatorname{Re}(\epsilon) \ll 1$, then the solutions $\mathbf{F}_{\mathrm{D}}$ of the corresponding lossless system are sufficiently good approximations to the solutions in the lossy device. Therefore, for small losses, we can apply the NEGF formulation in the previous section to Eq. (9) to compute the absorbed power:

$$\begin{aligned}P &= \int_0^{\infty} \frac{d\omega}{\pi}\omega \operatorname{Tr}\left[\operatorname{Im}\epsilon(\omega)\langle\mathbf{E}_{\mathrm{D}}\mathbf{E}_{\mathrm{D}}^{\dagger}\rangle_{\omega}\right] \\ &= \int_0^{\infty} \frac{d\omega}{\pi}\omega \operatorname{Tr}\left[\operatorname{Im}\epsilon(\omega)\sqrt{\epsilon_{\mathrm{R}}^{-1}}\langle\mathbf{F}_{\mathrm{D}}\mathbf{F}_{\mathrm{D}}^{\dagger}\rangle_{\omega}\sqrt{\epsilon_{\mathrm{R}}^{\dagger -1}}\right] \\ &\qquad\qquad (\text{using } \mathbf{F} = \sqrt{\epsilon_{\mathrm{R}}}\mathbf{E}) \\ &= \int_0^{\infty} \frac{d\omega}{\pi}\omega \operatorname{Tr}\left[\operatorname{Im}\epsilon(\omega)\sqrt{\epsilon_{\mathrm{R}}^{-1}}\mathbb{G}_{\mathrm{D}}\tau\langle\mathbf{F}_{\mathrm{I}}\mathbf{F}_{\mathrm{I}}^{\dagger}\rangle\tau^{\dagger}\mathbb{G}_{\mathrm{D}}^{\dagger}\sqrt{\epsilon_{\mathrm{R}}^{-1}}\right]\end{aligned} \tag{30}$$

where $\epsilon_{\mathrm{R}}^{\dagger} = \epsilon_{\mathrm{R}}$. Eq. (30) provides the power absorbed by the solar cell for incident solar radiation given by $\langle\mathbf{F}_{\mathrm{I}}\mathbf{F}_{\mathrm{I}}^{\dagger}\rangle$.

Using Eq. (30), we can compute the power absorbed by a solar cell in the presence of maximally concentrated sunlight, i.e. in the case of Fig. 1(c). Assuming the environment surrounding the cell to be a blackbody of temperature T at equilibrium, we have from the fluctuation-dissipation theorem [44],

$$\epsilon_0 \langle \mathbf{E}_\mathrm{I} \mathbf{E}_\mathrm{I}^\dagger \rangle_\omega = \mathrm{sgn}(\omega) \frac{2\hbar\omega^2/c^2}{e^{\hbar|\omega|/kT} - 1} \operatorname{Im} \mathbb{G}_\mathrm{S} = \pi\Theta(\omega) \Big[\frac{2\omega}{\pi c^2} \operatorname{Im} \mathbb{G}_\mathrm{S} \Big], \ \omega > 0 \tag{31}$$

where $\mathbb{G}_\mathrm{S}$ is the free-space Green's function that describes the surroundings, and $\Theta(\omega) = \hbar\omega/[e^{\hbar\omega/kT} - 1]$. Note that we are interested only in $\omega > 0$ from Eq. (30). We also note that to describe a realistic solar spectrum, one could use a form of $\Theta(\omega)$ different from the one used here without affecting the results that follow. Continuing from Eq. (30) we have

$$\begin{aligned} P &= \int_0^\infty \frac{d\omega}{\pi} \omega \operatorname{Tr} \Big[\operatorname{Im} \epsilon(\omega) \sqrt{\epsilon_\mathrm{R}^{-1}} \mathbb{G}_\mathrm{D} \tau \big[\pi\Theta(\omega) \frac{2\omega}{\pi c^2} \operatorname{Im} \mathbb{G}_\mathrm{S} \big] \tau^\dagger \mathbb{G}_\mathrm{D}^\dagger \sqrt{\epsilon_\mathrm{R}^{-1}} \Big] \\ &= \int_0^\infty d\omega \cdot \omega\Theta(\omega) \operatorname{Tr} \Big[\sqrt{\epsilon_\mathrm{R}^{-1}} \operatorname{Im} \epsilon(\omega) \sqrt{\epsilon_\mathrm{R}^{-1}} \cdot \frac{2\omega}{\pi c^2} \mathbb{G}_\mathrm{D} \tau \operatorname{Im} \mathbb{G}_\mathrm{S} \tau^\dagger \mathbb{G}_\mathrm{D}^\dagger \Big] & (32) \\ &= \int_0^\infty d\omega \cdot \omega\Theta(\omega) \operatorname{Tr} \Big[\sqrt{\epsilon_\mathrm{R}^{-1}} \operatorname{Im} \epsilon(\omega) \sqrt{\epsilon_\mathrm{R}^{-1}} \mathbb{A}_\mathrm{D}(\omega) \Big] & (33) \end{aligned}$$

where we used Eq. (28) to obtain Eq. (33). This result also tells us the optimal structure of the cell: from Eq. (29), maximum power absorption occurs when all modes in the device become 'accessible' to the environment. That is,

$$P_\mathrm{max} = \int_0^\infty d\omega \cdot \omega\Theta(\omega) \operatorname{Tr} \Big[\sqrt{\operatorname{Re} \epsilon^{-1}} \operatorname{Im} \epsilon(\omega) \sqrt{\operatorname{Re} \epsilon^{-1}} \mathbb{A}(\omega) \Big] \tag{34}$$

The derivations leading to Eqs. (33) and (34) represent the major new results of this paper. The results provide a rigorous derivation of the connection between the absorption under maximum concentration to the accessible density of states inside the device. This connection has been previously argued in Ref. [1] using the argument of detailed balance, assuming that the cell consists of a bulk medium. This connection has also been generalized in Refs. [28] and [31] for nanophotonic geometry. Neither of these papers, however, provide a rigorous derivation of this connection directly from Maxwell's equations. Our results here therefore provide a rigorous justification of the foundation of light trapping theory. In the next two sections we will explore the consequence of Eqs. (33)-(34). In Section V we provide a re-derivation of the standard light trapping results, starting from these equations.

We note that to arrive at Eq. (34), we make no assumption of the coupling between the free space and the device as described by the matrix τ, other than the assumption that all modes in the cell are accessible. Thus, Eq. (34) is equally applicable to a solar cell that has a Lambertian surface and hence absorbs and emits isotropically, as well as to a solar cell that has a strong angular selectivity. We will use this observation in Section V when we discuss the light trapping limit for a solar cell with a strong angular selectivity.

Before we discuss absorption enhancement, we would like to make a brief comment on spatial coherence of sunlight in the context of Eq. (31). In the formalism of fluctuational electrodynamics, which we use to obtain Eq. (31), the current-current correlation of the current source in the sun has the form

$$\langle \mathbf{J}(\mathbf{r}) \mathbf{J}^\dagger(\mathbf{r}') \rangle_\omega = \hbar\omega^2 \coth \frac{\hbar\omega}{2k_B T} \operatorname{Im} \epsilon(\mathbf{r}, \mathbf{r}) \cdot \delta(\mathbf{r} - \mathbf{r}') \tag{35}$$

That is, the current source in the sun is spatially incoherent. On the other hand, it is known that the sunlight is partially coherent [45, 46], and that coherence impacts device performance [47, 48]. We would like to point out here that our formalism, which builds upon fluctuational electrodynamics, takes spatial coherence into account in a systematic fashion because the field-field correlation of Eq. (31) is proportional to $\operatorname{Im} \mathbb{G}_\mathrm{S}$, which in general is not proportional to $\delta(\mathbf{r} - \mathbf{r}')$.

We also note that the derivation of Eq. (33) makes no use of reciprocity. Therefore, in Section VI we use these results to discuss light trapping in non-reciprocal structures.

V. ABSORPTION ENHANCEMENT

Various limits on absorption enhancement have been derived previously. The $4n^2$ limit in [1] was derived from a statistical thermodynamics and ray-tracing approach. This can be extended to a $4n^2/\sin^2\theta$ limit [3, 49] for the case of angle-selective emission from the solar cell. In addition, Ref. [8] considers the case of light trapping with a sub-wavelength grating, and concludes that at normal incidence that enhancement factor can significantly exceed the $4n^2$ limit. In this section, we briefly re-derive these limits starting from Eq. (34).

To derive the $4n^2$ limit, following Ref. [1], we consider a solar cell as described by a dielectric slab with a uniform dielectric constant $\epsilon = n^2 + i \cdot 2nn''$ such that $n''/n \ll 1$, where n and n'' are the real and imaginary parts of the refractive index, respectively. The absorption coefficient is $\alpha_0 = 2\,\mathrm{Im}(\omega\sqrt{\epsilon}/c) = 2\omega n''/c$. To start we assume that the device is under a full concentration of sun light, as shown in Fig. 1(c). To achieve light trapping in such a solar cell, one applies random roughness with a Lambertian profile on the surface of the solar cell, which allows all modes in the device to be accessible. As a result we can use Eq. (34) to compute the absorption in the cell. For such a slab $\mathrm{Tr}\,\mathbb{A} = L^2 d \cdot n^3\omega^2/\pi^2 c^3$. With $\epsilon''/\epsilon' = 2n''/n$ and $\Theta(\omega) = \hbar\omega/(\exp(\hbar\omega/k_B T) - 1)$, the absorbed power in a narrow frequency range between ω and $\omega + \Delta\omega$ is then,

$$\begin{aligned} P_{\max} &= \frac{\hbar\omega}{e^{\hbar\omega/k_B T} - 1}\frac{2\omega n''}{n}\frac{n^3\omega^2}{\pi^2 c^3}\Delta\omega L^2 d \\ &= 2n^2\alpha_0 d \cdot \left[\frac{\omega^2\Delta\omega}{4\pi^2 c^2} \cdot \frac{\hbar\omega}{e^{\hbar\omega/k_B T} - 1} \cdot 2L^2\right] \end{aligned} \quad (36)$$

where the quantity in the brackets is the well-known formula for power from isotropic blackbody radiation, incident in this case on a surface of area of $2L^2$. With the bracketed quantity as the input power P_{in}, the maximum enhancement is

$$f = \frac{1}{\alpha_0 d}\frac{P_{\max}}{P_{in}} = 2n^2 \quad (37)$$

The standard result of $4n^2$ corresponds to the case where a perfect rear reflector is placed with the source only incident from the upper half hemisphere. Because of the reflector, the absorbed power remains the same; but the incident power is only a half of the isotropic radiation:

$$f = \frac{1}{\alpha_0 d}\frac{P_{\max}}{P_{in}/2} = 4n^2 \quad (38)$$

The commonly derived limit of $4n^2$ corresponds to a single incident mode on a solar cell with a Lambertian surface. However, since a Lambertian surface results in equal absorption from all incident modes, the absorbed power as well as the incident power are scaled by the same factor in going from isotropic illumination to a single incident mode. In other words, the absorption enhancement factor remains unaffected by the angular range of incident radiation on a solar cell with a Lambertian surface.

The derivation above can be generalized to describe a solar cell with strong angular selection. As an illustration, we consider a solar cell that has equal absorption for light within the absorption cone having an angle of incidence within a range θ around the normal direction, and has zero absorption for incident light outside the absorption cone. In this case, assuming all modes within the cell is accessible, under full concentration the absorption of solar cell is described by Eq. (36). On the other hand, since the incident light outside the absorption cone does not contribute to the solar cell absorption, the absorption remains unchanged if we restrict the incident radiation to only within the absorption cone. That is, the absorption remains unchanged even when the incident radiation is reduced to $P_{in} = [\omega^2\Delta\omega/4\pi^2c^2]\Theta(\omega)\sin^2\theta$, which leads to the limit of $4n^2/\sin^2\theta$.

Ref. [8] considered the case where the light trapping is accomplished by placing a grating with a sub-wavelength periodicity on the surface of solar cell, and showed that in this case the enhancement factor can significantly exceed $4n^2$ for normally incident light. This increased enhancement factor arises due to angle-selectivity of the grating structure in the single-channel regime, and comes at the expense of lower enhancement at large angles [8] since the total enhancement integrated across all angles is constrained for any solar cell structure [50]. This is in contrast with the scheme of Refs. [28, 51], where an enhancement factor exceeding $4n^2$ for all angles of incidence were achieved in a thin, low-index absorber surrounded by high-index media. We re-derive the result of Ref. [8] for normal incidence using the formalism developed in Section IV. When the grating period is less than the free-space wavelength, normally incident light cannot scatter into any other directions aside from normal. Therefore, the surrounding medium can be described as a one-dimensional system. In using Eq. (31) to describe the incident light, one needs to use an expression for $\mathrm{Im}\,\mathbb{G}_{\mathrm{S}}$ that is appropriate for the one-dimensional system. With this modification, the derivation to Eq. (36) remains unchanged. That is, assuming that all modes in the cell are accessible, the power absorbed by the cell is

$$P_{\max} = 4n^2\alpha_0 d \cdot \left[\frac{\omega^2\Delta\omega}{4\pi^2 c^2} \cdot \frac{\hbar\omega}{e^{\hbar\omega/k_B T} - 1} \cdot l^2\right] \quad (39)$$

where l is the periodicity of the patterning on the top surface. On the other hand, the incident power changes from its 3D expression of $\Theta(\omega) \cdot \omega^2\Delta\omega/4\pi^2c^2 \cdot l^2$ to the 1D expression of $\Theta(\omega) \cdot \Delta\omega/\pi$, where we used the fact that the 1D density of states is $\Delta\omega/\pi c$. Therefore, the

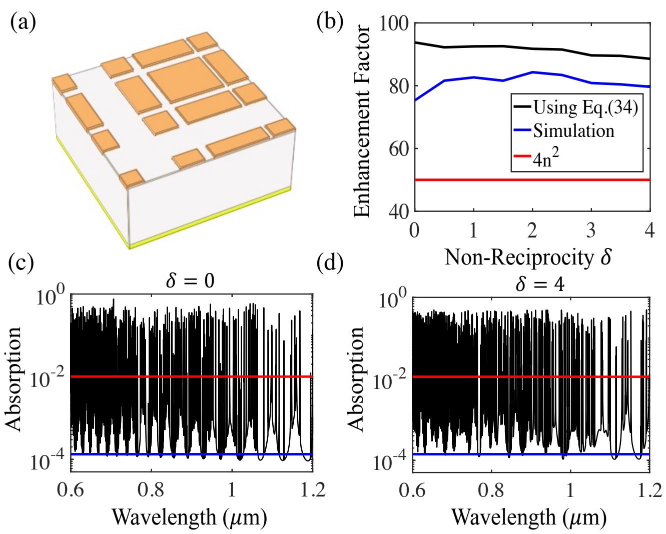

FIG. 3. (a) One unit cell of the solar cell structure considered, with a back-reflector (yellow). The unit cell is a square with side length $l = 600$ nm, which also corresponds to the periodicity of the structure. The thickness of the bulk absorbing material (grey) is $d = 3$ μm. The orange regions are non-absorbing dielectric material. The air slots between the orange regions have widths that are 20%, 5% and 2% of the period along one direction, and 20%, 5% and 6% of the period along the other. The thickness of the patterning region is 50 nm. (b) Enhancement factor as a function of the strength of non-reciprocity. The black solid curve was obtained using Eq. (34), which presents the theoretical upper limit of enhancement. The blue curve is the result of our numerically obtained absorption enhancement averaged over the wavelength range of interest and over the two polarizations. The $4n^2$ limit is shown in red for reference. (c) and (d) Absorption spectra with spectrally averaged absorption, i.e. $\bar{f}(\delta)\alpha_0(\delta)d$ (red) and single-pass absorption, i.e. $\alpha_0(\delta)d$ (blue) for $\delta = 0$ and $\delta = 4$ respectively.

enhancement factor in this scenario is modified from the expression in Eq. (38) to

$$f = 4n^2 \cdot \frac{\Theta(\omega)\frac{\omega^2\Delta\omega}{4\pi^2c^2} \cdot l^2}{\Theta(\omega) \cdot \frac{\Delta\omega}{\pi}} = 4\pi n^2 s^2 \tag{40}$$

where $s = l/\lambda$.

VI. LIGHT TRAPPING IN NON-RECIPROCAL SYSTEMS

In the previous section we used the NEGF formalism to reproduce the standard theoretical results for solar cell light trapping. As noted in Section IV, however, our result here is in fact more general as compared to previous theoretical work on solar cell light trapping in that we do not make assumption on reciprocity. This is in contrast to all previous theoretical works in this area. For example, Ref. [1] assumes detailed balance in order to reach a conclusion similar to Eq. (33). Detailed balance is a consequence of reciprocity. In Ref. [28], results similar to Eq. (33) were derived using the temporal coupled mode theory formalism, which again assumes reciprocity. In our work here, by re-deriving all these previous results in Section V, we have in fact shown that these results are equally applicable to a cell containing non-reciprocal materials.

The potential of using non-reciprocal material for solar energy conversion is a subject that is of fundamental interest. It is known that the Landsberg limit, which represents the upper limit of solar energy conversion, can only be reached with the use of non-reciprocal materials [52–55]. On the other hand, it is also known that the reciprocity between emission and absorption can be broken with the use of magneto-optical media, and such a reciprocity breaking can be further enhanced with the use of nanophotonic structures [56, 57]. These results raise the question as to how breaking reciprocity affects the light trapping limit. Since Eq. (34) is applicable for both reciprocal and non-reciprocal cases, our results show that as long as the accessible density of states within the solar cell is the same, the upper limit of light trapping enhancement should not be affected by reciprocity-breaking.

We validate the theoretical results above using numerical simulations. For the absorber we consider a slab of a non-reciprocal material. The slab has a thickness of 3 micron. The dielectric constant of such a material is in general asymmetric, i.e. $\epsilon^T \neq \epsilon$. As an illustration, we choose the following form [58]:

$$\epsilon = \begin{pmatrix} (n+i\kappa)^2 & i\delta & 0 \\ -i\delta & (n+i\kappa)^2 & 0 \\ 0 & 0 & (n+i\kappa)^2 \end{pmatrix} \tag{41}$$

where $n^2 = 12.5$. δ characterizes the strength of the non-reciprocity, with $\delta = 0$ describing the reciprocal material. The loss κ is chosen such that the absorption length α_0^{-1} in the reciprocal case of $\delta = 0$ equals $(2\omega\kappa(\omega)/c)^{-1} = 22.5$ mm over the wavelength range of interest. For typical magneto-optical materials, the maximum δ/n^2 is typically $< 10^{-2}$ (see for e.g. Refs. [59, 60]). In our numerical simulation, however, to explore the effect of non-reciprocity, we consider a much wider range δ from 0 to 4.

To achieve light trapping in such an absorbing layer, we place a perfect electric conductor mirror at the bottom of the layer (yellow layer, Fig. 3(a)). On the top surface we place a grating layer (orange) following Ref. [8]. The grating layer consists of several rectangle-shaped dielectric regions with dielectric constant of n^2, separated by air slots. The grating layer has a thickness of 50 nm. The periodicity l of the grating is chosen to be 600 nm on both in-plane directions. We consider a wavelength λ ranging from 600 nm to 1200 nm. The pattern of the grating is such that there is not any mirror or rotational symmetry within the plane. This choice of periodicity and the use of such an asymmetric grating pattern ensure that there is not any uncoupled mode in the slab due to either translational symmetry or point-group symmetry considerations, in our wavelength range of interest.

Within our wavelength range of interest the cell operates at the single channel regime [28], where for normally incident light in this regime there is only zero-th order diffraction in the air region outside the cell. For the reciprocal case of $\delta = 0$, the theoretical upper-limit of absorption enhancement in this wavelength range is given by Eq. (40) where $s = l/\lambda$ takes values between 0.5 and 1. Therefore, the spectrally averaged absorption enhancement over this wavelength range is

$$\bar{f}_{\mathrm{TH}} = \frac{1}{\omega_{\mathrm{R}} - \omega_{\mathrm{L}}} \int_{\omega_{\mathrm{L}}}^{\omega_{\mathrm{R}}} 4\pi n^2 s^2 \cdot \mathrm{d}\omega = 4\pi \cdot \frac{7}{12} \cdot n^2 \approx 91.6 \tag{42}$$

Following the same derivation that leads to Eq. (40), the light trapping enhancement factor for the non-reciprocal case can be derived as:

$$\bar{f}_{\mathrm{TH}}(\delta) = \frac{1}{\omega_{\mathrm{R}} - \omega_{\mathrm{L}}} \int_{\omega_{\mathrm{L}}}^{\omega_{\mathrm{R}}} \frac{P_{\max}(\omega, \delta)}{\alpha_0(\delta) d \cdot \Theta(\omega) \cdot \Delta\omega/\pi} \mathrm{d}\omega \tag{43}$$

as shown by the black solid curve in Fig. 3(b). Here $\alpha_0(\delta)$ is the single-pass absorption length for normally propagating light in the non-reciprocal material. The theoretical results show that the light trapping enhancement factor is largely independent of δ, in spite of the large range of δ that we have used. We note that with our choice of a fairly sizable range of δ, the density of states does depend on δ. This dependency, however, is largely cancelled out by the dependency of the group velocity on δ.

As a validation of the theoretical results, we perform a numerical simulation (blue dotted curve) using S^4 [61], an electromagnetic solver for layered media based on the method of Rigorous Coupled Wave Analysis (RCWA). We vary the strength of non-reciprocity by changing δ between 0 and 4, and compute for each case the enhancement

$$\bar{f}(\delta) = \frac{1}{\omega_{\mathrm{R}} - \omega_{\mathrm{L}}} \int_{\omega_{\mathrm{L}}}^{\omega_{\mathrm{R}}} \frac{a(\omega)}{\alpha_0(\delta) d} \mathrm{d}\omega \tag{44}$$

where $a(\omega)$ is the spectrum of the absorption coefficient, averaged across polarizations. Fig. 3(c)-(d) show such spectra for the cases of $\delta = 0$ and $\delta = 4$ respectively. The red curve in Fig. 3(b) serves as a reference level corresponding to the $4n^2$ enhancement of the single-pass absorption. We note that in consistency with the theoretical results, the simulated enhancement $\bar{f}$ varies only slightly for a large variation in the non-reciprocity δ. The simulation supports our claim based on Eq. (34) that the maximum possible enhancement is set by the DOS of the material, and is unaffected by the breaking of reciprocity. The simulated enhancement $\bar{f}$ in all cases remains below the theoretical upper-limit $\bar{f}_{\mathrm{TH}}$, because at the chosen absorption length, some modes are not in the over-coupling regime, where the external coupling is much greater than the intrinsic loss rate [8]. In the formalism developed here, this means that the accessible density of states $\mathbb{A}_{\mathrm{D}}$ is smaller than the density of states $\mathbb{A}$ of the isolated cell.

VII. NON-NEGLIGIBLE LOSS

In this section, we extend the discussion of the NEGF formulation to solar cells whose loss is not infinitesimal. The wave equation upon combining Eq. (11)–Eq. (14) is

$$\nabla \times \nabla \times \mathbf{E}(\omega) = \frac{\omega^2}{c^2} \epsilon(\omega) \mathbf{E}(\omega) \tag{45}$$

A non-Hermitian $\epsilon(\mathbf{r}, \omega)$ can in principle have many square roots $\sqrt{\epsilon(\mathbf{r}, \omega)}$; however, any choice of the square root will mathematically give the same power absorption, since Eq. (9) depends only on $\epsilon(\mathbf{r}, \omega)$ and $\mathbf{E}(\mathbf{r}, \omega)$. Further, we neglect material dispersion again by considering a narrow frequency range.

Choosing one such square root $\sqrt{\epsilon(\mathbf{r})}$, we have

$$\mathbb{H}\mathbf{F} \equiv \left[\sqrt{\epsilon^{-1}} \nabla \times \nabla \times \sqrt{\epsilon^{-1}}\right] \mathbf{F} = \frac{\omega^2}{c^2} \mathbf{F} \tag{46}$$

where the 'Hamiltonian' $\mathbb{H}$ is no longer Hermitian. $\mathbb{H}$ can still be decomposed in a manner similar to Eq. (16) as

$$\mathbb{H} = \begin{pmatrix} \mathbb{H}_{\mathrm{S}} & \tau_1 \\ \tau_2 & \mathbb{H}_{\mathrm{D}} \end{pmatrix} \tag{47}$$

The cross-terms τ_1 and τ_2 correspond to the cell boundaries, and we make a simplifying assumption that the non-Hermiticity arising from Eq. (46) is captured purely in the bulk of the cell, i.e. $\tau_2 = \tau_1^\dagger = \tau$ but $\mathbb{H}_{\mathrm{D}}^\dagger \neq \mathbb{H}_{\mathrm{D}}$. The Hamiltonian for the environment, $\mathbb{H}_{\mathrm{S}}$, remains Hermitian since it is unaffected by the dielectric function of the cell $\epsilon(\mathbf{r})$.

The relations given by Eqs. (19)-(21) continue to hold for the non-Hermitian $\mathbb{H}_{\mathrm{D}}$. By defining the spectral function $\mathbb{A}_{\mathrm{D}}$ as in Eq. (26), we observe a departure from Eq. (27)

$$\begin{aligned} \mathrm{Im}\, \mathbb{G}_{\mathrm{D}} &= \frac{\mathbb{G}_{\mathrm{D}} - \mathbb{G}_{\mathrm{D}}^\dagger}{2i} \\ &= \mathbb{G}_{\mathrm{D}} \frac{\mathbb{G}_{\mathrm{D}}^{\dagger -1} - \mathbb{G}_{\mathrm{D}}^{-1}}{2i} \mathbb{G}_{\mathrm{D}}^\dagger \\ &= \mathbb{G}_{\mathrm{D}} [\mathrm{Im}\, \Sigma] \mathbb{G}_{\mathrm{D}}^\dagger + \mathbb{G}_{\mathrm{D}} [\mathrm{Im}\, \mathbb{H}_{\mathrm{D}}] \mathbb{G}_{\mathrm{D}}^\dagger \\ &= \mathbb{G}_{\mathrm{D}} \tau [\mathrm{Im}\, \mathbb{G}_{\mathrm{S}}] \tau^\dagger \mathbb{G}_{\mathrm{D}}^\dagger + \mathbb{G}_{\mathrm{D}} [\mathrm{Im}\, \mathbb{H}_{\mathrm{D}}] \mathbb{G}_{\mathrm{D}}^\dagger \end{aligned} \tag{48}$$

where the first term on the right hand side is the same as Eq. (27). The second term corresponds to material loss. In the limit of the lossless system, we see that Eq. (48) reduces to Eq. (27) as $\operatorname{Im}\mathbb{H}_{\mathrm{D}} \to 0$. Inserting this relation, rearranged as $\mathbb{G}_{\mathrm{D}}\tau[\operatorname{Im}\mathbb{G}_{\mathrm{S}}]\tau^{\dagger}\mathbb{G}_{\mathrm{D}}^{\dagger} = \operatorname{Im}\mathbb{G}_{\mathrm{D}} - \mathbb{G}_{\mathrm{D}}[\operatorname{Im}\mathbb{H}_{\mathrm{D}}]\mathbb{G}_{\mathrm{D}}^{\dagger}$, in Eq. (32), we get

$$
\begin{aligned}
P &= \int_0^{\infty} d\omega \cdot \omega\Theta(\omega) \operatorname{Tr}\left[\left(\sqrt{\epsilon^{\dagger}}\right)^{-1} \operatorname{Im}\epsilon(\omega)\sqrt{\epsilon^{-1}} \cdot \frac{2\omega}{\pi c^2}\mathbb{G}_{\mathrm{D}}\tau \operatorname{Im}\mathbb{G}_{\mathrm{S}}\tau^{\dagger}\mathbb{G}_{\mathrm{D}}^{\dagger}\right] \\
&= \int_0^{\infty} d\omega \cdot \omega\Theta(\omega) \operatorname{Tr}\left[\left(\sqrt{\epsilon^{\dagger}}\right)^{-1} \operatorname{Im}\epsilon(\omega)\sqrt{\epsilon^{-1}} \cdot \frac{2\omega}{\pi c^2}\operatorname{Im}\mathbb{G}_{\mathrm{D}}\right] - \int_0^{\infty} d\omega \cdot \omega\Theta(\omega) \operatorname{Tr}\left[\left(\sqrt{\epsilon^{\dagger}}\right)^{-1} \operatorname{Im}\epsilon(\omega)\sqrt{\epsilon^{-1}} \cdot \frac{2\omega}{\pi c^2}\mathbb{G}_{\mathrm{D}}[\operatorname{Im}\mathbb{H}_{\mathrm{D}}]\mathbb{G}_{\mathrm{D}}^{\dagger}\right] \\
&= \int_0^{\infty} d\omega \cdot \omega\Theta(\omega) \operatorname{Tr}\left[\left(\sqrt{\epsilon^{\dagger}}\right)^{-1} \operatorname{Im}\epsilon(\omega)\sqrt{\epsilon^{-1}}\mathbb{A}_{\mathrm{D}}\right] - \int_0^{\infty} d\omega \cdot \omega\Theta(\omega) \operatorname{Tr}\left[\left(\sqrt{\epsilon^{\dagger}}\right)^{-1} \operatorname{Im}\epsilon(\omega)\sqrt{\epsilon^{-1}} \cdot \frac{2\omega}{\pi c^2}\mathbb{G}_{\mathrm{D}}[\operatorname{Im}\mathbb{H}_{\mathrm{D}}]\mathbb{G}_{\mathrm{D}}^{\dagger}\right]
\end{aligned} \tag{49}
$$

where $\mathbb{A}_{\mathrm{D}} \equiv (2\omega/\pi c^2)\operatorname{Im}\mathbb{G}_{\mathrm{D}}$ as before. The result here indicates that due to the second term on the right, the enhancement factor decreases as the material absorption strength increases, in consistency with the derivation [30] from statistical-temporal coupled mode theory.

VIII. CONCLUSION

In this paper, we derived a theory of light-trapping in solar cells based on the Non-Equilibrium Green's Function formalism applied to Maxwell's Equations. The theory provides a rigorous connection between light-trapping and the accessible density of states of the cell, in the form of an upper bound on the power absorbed by the cell. The derived upper bound was used to obtain the standard light-trapping results involving Lambertian cells or periodic patternings. Further, since the theory was derived without the assumption of reciprocity, the upper bound on absorption was applicable to non-reciprocal cells, showing that the standard light-trapping enhancement cannot be overcome by breaking reciprocity alone. This result was numerically tested and verified on a slab-like cell with periodic patterning, where it was seen that the enhancement was largely independent of non-reciprocity for wide range of parameters. Our results here provide a rigorous theoretical foundation for the light trapping of solar cells. In addition, the development points to the potential significance of the Non-Equilibrium Green's Function (NEGF) formalism in the treatment of solar and thermal radiation problems.

This work is supported by the U. S. Department of Energy Grant No. DE-FG-07ER46426. Siddharth Buddhiraju in addition acknowledges the support of a Stanford Graduate Fellowship.

[1] E. Yablonovitch, Journal of the Optical Society of America **72**, 899 (1982).
[2] A. Goetzberger, in *15th Photovoltaic Specialists Conference* (1981), pp. 867–870.
[3] P. Campbell and M. A. Green, IEEE Transactions on Electron Devices **33**, 234 (1986).
[4] P. Campbell and M. A. Green, Journal of Applied Physics **62**, 243 (1987).
[5] C. Heine and R. H. Morf, Applied Optics **34**, 2476 (1995).
[6] M. A. Green, Progress in Photovoltaics: Research and Applications **10**, 235 (2002).
[7] A. Chutinan, N. P. Kherani, and S. Zukotynski, Optics Express **17**, 8871 (2009).
[8] Z. Yu, A. Raman, and S. Fan, Optics Express **18**, A366 (2010).
[9] E. Garnett and P. Yang, Nano Letters **10**, 1082 (2010).
[10] M. D. Kelzenberg, S. W. Boettcher, J. A. Petykiewicz, D. B. Turner-Evans, M. C. Putnam, E. L. Warren, J. M. Spurgeon, R. M. Briggs, N. S. Lewis, and H. A. Atwater, Nature Materials **9**, 239 (2010).
[11] H. A. Atwater and A. Polman, Nature Materials **9**, 205 (2010).
[12] R. A. Pala, J. White, E. Barnard, J. Liu, and M. L. Brongersma, Advanced Materials **21**, 3504 (2009).
[13] C. Battaglia, C.-M. Hsu, K. Soderstrom, J. Escarre, F.-J. Haug, M. Charriere, M. Boccard, M. Despeisse, D. T. Alexander, M. Cantoni, et al., ACS Nano **6**, 2790 (2012).
[14] K. X. Wang, Z. Yu, V. Liu, Y. Cui, and S. Fan, Nano Letters **12**, 1616 (2012).
[15] D. Zhou and R. Biswas, Journal of Applied Physics **103**, 093102 (2008).
[16] H. Tan, R. Santbergen, A. H. Smets, and M. Zeman, Nano Letters **12**, 4070 (2012).
[17] M. A. Green and S. Pillai, Nature Photonics **6**, 130 (2012).
[18] P. Spinelli, V. Ferry, J. Van de Groep, M. Van Lare, M. Verschuuren, R. Schropp, H. Atwater, and A. Polman, Journal of Optics **14**, 024002 (2012).
[19] S. E. Han and G. Chen, Nano Letters **10**, 4692 (2010).
[20] S. B. Mallick, M. Agrawal, and P. Peumans, Optics Express **18**, 5691 (2010).
[21] S. Mokkapati and K. Catchpole, Journal of Applied

Physics **112**, 101101 (2012).
[22] C. Rockstuhl, S. Fahr, and F. Lederer, Journal of Applied Physics **104**, 123102 (2008).
[23] V. E. Ferry, A. Polman, and H. A. Atwater, ACS Nano **5**, 10055 (2011).
[24] M. A. Green, IEEE Transactions on Electron Devices **31**, 671 (1984).
[25] T. Tiedje, E. Yablonovitch, G. D. Cody, and B. G. Brooks, IEEE Transactions on Electron Devices **31**, 711 (1984).
[26] H. R. Stuart and D. G. Hall, Journal of the Optical Society of America A **14**, 3001 (1997).
[27] H. R. Stuart and D. G. Hall, Applied Physics Letters **73**, 3815 (1998).
[28] Z. Yu, A. Raman, and S. Fan, Proceedings of the National Academy of Sciences **107**, 17491 (2010).
[29] Z. Yu and S. Fan, Applied Physics Letters **98**, 011106 (2011).
[30] Z. Yu, A. Raman, and S. Fan, Physical Review Letters **109**, 173901 (2012).
[31] D. M. Callahan, J. N. Munday, and H. A. Atwater, Nano Letters **12**, 214 (2012).
[32] H. A. Haus, *Waves and Fields in Optoelectronics* (Prentice-Hall,, 1984).
[33] S. Fan, W. Suh, and J. Joannopoulos, Journal of the Optical Society of America A **20**, 569 (2003).
[34] W. Suh, Z. Wang, and S. Fan, IEEE Journal of Quantum Electronics **40**, 1511 (2004).
[35] S. Datta, *Quantum Transport: Atom to Transistor* (Cambridge University Press, 2005).
[36] S. Datta, Superlattices and Microstructures **28**, 253 (2000).
[37] E. Yablonovitch and G. D. Cody, IEEE Transactions on Electron Devices **29**, 300 (1982).
[38] J. D. Jackson, *Classical Electrodynamics* (Wiley Online Library, 1998), 3rd ed.
[39] P. Sheng, IEEE Transactions on Electron Devices **31**, 634 (1984).
[40] A. Raman and S. Fan, Physical Review Letters **104**, 087401 (2010).
[41] J. D. Joannopoulos, S. G. Johnson, J. N. Winn, and R. D. Meade, *Photonic Crystals: Molding the Flow of Light* (Princeton University Press, 2011).
[42] S. Datta, *Electronic transport in mesoscopic systems* (Cambridge University Press, 1997).
[43] A. Lagendijk and B. A. Van Tiggelen, Physics Reports **270**, 143 (1996).
[44] W. Eckhardt, Physical Review A **29** (1984).
[45] M. E. Verdet, *Leçons d'optique physique*, vol. 1 (Masson, 1869).
[46] S. Divitt and L. Novotny, Optica **2**, 95 (2015).
[47] H. Alaibakhsh and G. Darvish, Applied Optics **55**, 1808 (2016).
[48] A. Herman, M. Sarrazin, and O. Deparis, New Journal of Physics **16**, 013022 (2014).
[49] E. D. Kosten, J. H. Atwater, J. Parsons, A. Polman, and H. A. Atwater, Light: Science & Applications **2**, e45 (2013).
[50] Z. Yu and S. Fan, Applied Physics Letters **98**, 011106 (2011).
[51] M. A. Green, Progress in Photovoltaics: Research and Applications **19**, 473 (2011).
[52] P. Landsberg and G. Tonge, Journal of Applied Physics **51**, R1 (1980).
[53] H. Ries, Applied Physics B **32**, 153 (1983).
[54] M. A. Green, Nano Letters **12**, 5985 (2012).
[55] A. Polman and H. A. Atwater, Nature Materials **11**, 174 (2012).
[56] L. Zhu and S. Fan, Physical Review B **90**, 220301 (2014).
[57] D. A. Miller, L. Zhu, and S. Fan, Proceedings of the National Academy of Sciences **114**, 4336 (2017).
[58] P. Pershan, Journal of Applied Physics **38**, 1482 (1967).
[59] K. Fang, Z. Yu, V. Liu, and S. Fan, Optics Letters **36**, 4254 (2011).
[60] V. Belotelov, I. Akimov, M. Pohl, V. Kotov, S. Kasture, A. Vengurlekar, A. V. Gopal, D. Yakovlev, A. Zvezdin, and M. Bayer, Nature Nanotechnology **6**, 370 (2011).
[61] V. Liu and S. Fan, Computer Physics Communications **183**, 2233 (2012).